International Journal of Nanoelectronics and Materials
Volume 15, No. 2, April 2022 [177-188]

Optimization of SPR Brass-layer Aquatic Sensor's Sensitivity by Simulation

Mirvat Dawood Majed[1] , Ruqayah A. Ulwali[1*], Heba Kh. Abbas [1], Ali A. Al-Zuky [2], Anwar H. Al-Saleh [3]

[1]University of Baghdad , College of Science for Women , Department of Physics ,Baghdad, Iraq
[2]Mustansiriya University, College of Science, Department of Physics , Baghdad , Iraq
[3]Mustansiriya University, College of Science , Department of Computer Science, Baghdad , Iraq

Received 16 June 2021, Revised 4 January 2022, Accepted 8 March 2022

ABSTRACT

The Fresnel equations of reflectivity of electromagnetic wavelengths in the range of 100nm to 1000nm were adopted in this work, and a simulation program was constructed using MATLAB b2018 based on the transfer matrix for a three-layer system. The layers are FD60_Dense flint prism, brass variable thickness layer (10 - 80) nm with step changes 10nm, and water layer, for improving the sensitivity of (SPR) sensor based Kretschmann's configuration. Numerical results have demonstrated that there is no surface plasmon resonance sensor within the range of wavelengths (100 – 500) nm, while it appears weak in visible region and well in (IR) region at wavelengths (900 and 1000) nm. The phenomenon of SPR begins to gradually weaken with the increasing brass layer thickness. Also, the Full width at Half Maximum (FWHM) is decrease with increased brass layer thickness and SPR dip length (H). While the best values obtained for sensitivity were in the visible region at the wavelength of 700nm, where it was almost stable with an increase in the thickness of the brass layer from 20nm to 50nm and with values higher than 115 deg/RIU. But in the infrared region, the sensitivity was between (100 to 103) deg/RIU and almost stable for brass layer thicknesses from about 20nm to 60nm. No previous study has examined this wide range of wavelengths. Through the simulation, we were able to determine the best range of wavelengths that can be used for the purpose of designing an aqueous or biological sensor based on the brass layer with a thickness between 40 nm to 50 nm.

Keywords: Surface plasmon resonance sensor, brass layer, Kretschmann's configuration

1. INTRODUCTION

The plasmon surface resonance occurs when the incident light's resonance matches the surface pulse, thus the (SPR) effect is defined as the surface plasmon wave by exponentially degenerate temporal area for incident p-polarized ray, under this condition the resonance is content (Ghosh and Ray, 2015 ; Shukla et al., 2015).The SPR phenomenon was used widely in different subjects area for instance, sensor technology, optical modulators, nonlinear optics, microscopy and spectroscopy (Srivastava et al., 2011; Robertson and May, 1999) . Through the another three decades , There was an attention in the subject of surface plasmon resonance sensing technology according to its advantages such as elevation sensitivity, actual time and high exposure accuracy (Shukla et al., 2015 ; Su et al., 2013). One of the most important factors affecting the performance for a surface plasmon resonance (SPR) sensor is

*Corresponding author: ruqayah.a@csw.uobaghdad.edu.iq

the detection sensitivity because it will determine the sensor's ability to detect the type and concentration of the sample (Wang et al., 2014) .

A significant difference in resonance angle in phase interrogation or resonant wavelength (wavelength interrogation) is achieved to achieve high sensitivity, and sample parameters such as refractive index, thickness and concentration (Kita et al., 2009). The resonance sensor for surface Plasmon refers to variations under the medium refractive index (the analytes), in which the sensor surface is in direct contact. Any disruption leading to a reduction in a material's refractive index may be analyzed using SPR sensors. The main factors which change the value of a medium's refractive index are: optical interaction, absorption, defects, biological processes, etc. A variation in the resolution angle with almost total loss at relative strength of completely reflected light may be investigated by the monitoring or by a change in the decay period of evanescent fields related to Plasmon polar tons. The sensor's responses can be examined.

There are several studies used to develop SPR sensors and improve their sensitivity by additional layers of semiconductor, dielectric, or metamaterials: Graphene sheets were used by Xu et al., 2016 to enhance SPR and prevent oxidation. Their proposed SPR sensor was shown to be 3.4 times more sensitive than an Al-based sensor without a graphene layer. Fouad et al. ; (2016) investigated the surface plasmon resonance sensor phase interrogation technique based on the silver and thin film insulating film of barium titanate layers. Their numerical results demonstrated that the proposed BaTiO3 layer fusion into the surface plasmon resonance sensor results in a higher sensitivity of 280 ° / RIU compared to the surface plasmon resonance sensor without a layer BaTiO3 that only shows 120 ° / RIU sensitivity.

By interrogating technology, Fouad et al. (2017) applied a layer of gold (50 nm) and a thin layer of barium titanate (BaTio3) (5 nm) to improve the sensitivity of the SPR sensor. Their results reveal that using BaTio3 improved sensitivity from (160°/ RIU) to (250°/ RIU) when compared to not using BaTio3.

Through the (Au and Ni) films, Nisha et al. (2019) applied a layer of MoS2 sandwich. They discovered that adding graphene to the Ni film improved the sensitivity to 229°/RIU. They also noticed that the sensitivity of the proposed sensor changes as the number of graphene and MoS2 layers increases.

In Lin et al. (2020), they presented an SPR sensor that uses a hybrid structure of two-dimensional materials (graphene, MoS2, WS2, and WSe2) and metal layers (Au, Ag, or Cu) to achieve the highest sensitivity for a certain wavelength of incident light using genetic algorithms. They discovered that the sensitivity of the suggested sensor using Ag layer varied widely with changing incident ray wavelength and improved numerically to 194°/RIU when compared to Au(159°/RIU) and Cu(155°/RIU).

Kadhum, F.J et al. (2021) designed a bimetallic surface plasmon resonance (SPR) sensor from a simulation model at different thicknesses of the titanium oxide (TiO_2) (d_{TiO2}=50nm) and silver (Ag) (d_{Ag}=10-80nm) layers, which are deposited on the semicircular glass prism D-ZLAF50 by using the water as a sensing medium. The surface plasmon resonance angle (θ_{SPR}) properties are calculated, SPR are appeared strongly well in the visible region at (600,700) nm and in the infrared region (900,1000) nm too. The best sensitivity (S=140) can be observed in the visible region, where the values of SPR dip length (Ld) and full width half maximum (FWHM) are very good at silver layer thicknesses (40-60nm), therefore the proposed sensor can be used in the visible and infrared regions at the wavelengths (600, 700, 900, and 1000) nm.

In this study, a plasmonic resonance simulation of brass thin layers that were deposited on a semicircular prism is performed. Then, the study of sensor sensitivity as a function of any slight variation in the value of the refractive index of the sensitivity medium and for a wide range of wavelengths of incident light from 100nm to 1000nm with a control of the thickness of brass layer from 10nm to 80nm were conducted.

2. SURFACE PLASMON RESONANCE (SPR) THEORY

The procedure for the resonance excitation of the surface wave Plasmon, as seen in Figure 1, was employed to explain the phenomenon of (SPR), attenuated total reflection (ATR) cuppler method (Fouad et al., 2017). The single configuration is Otto kind where the dielectric constant sensor ε_d between the prism and the layer of metal has dielectric ε_m constant like Au or Ag on the surface of the Plasmon Wave is enclosed in this setting. If the incident light beam is at an angle (Θ), equivalent to the critical angle the internal total reflection takes place between the prism and the sensor layer, the time area.

The other type of structure of this type is Kretschmann, the dielectric constant of the sensitivity medium, a specifically deposited metallic film that is protected by the metal sheet. The light-ray still illuminates the prism in an event angle (Θ) greater than the critic angle, as that the whole inner reflection takes place on the prism/metal interface. The temporary ray of the whole inner reflection penetrates into the metal surface which causes the plasmon wave to spread across the interface between metal and sensing. This scheme is used for most experimental applications, such that sensing medium gaps do not have to be regulated in comparison with Otto form (Maharana et al., 2014).

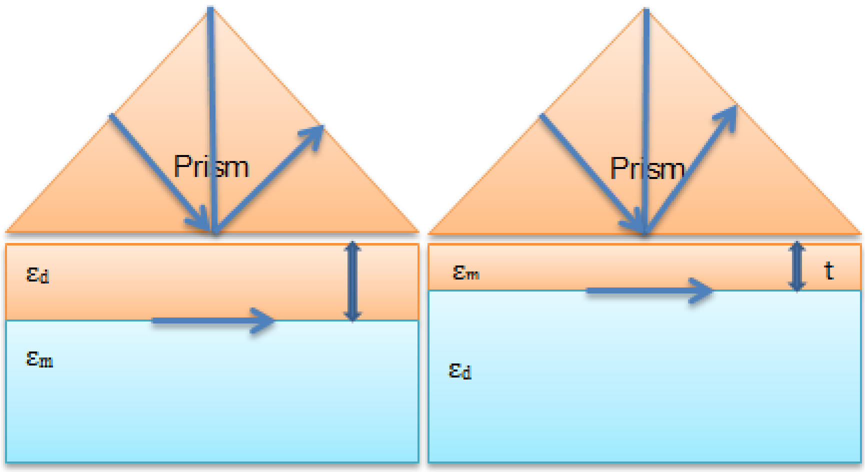

Figure 1. Surface Plasmon Sensor arrangement : (a) Otto type (b) Kretschmann type

The state of the resonance is fulfilled by adjusting the P-polarized incident light vector matches the surface plasmon wave's vector, which spreads around the metal sensing medium interface:

$$K = K_{spr} \quad .... (1)$$

where K is the incident wave light vector and K_{spr} is the surface Plasmon wave vector. Theseparameters are given by:

$$K = \frac{2\pi}{\lambda} n_p \times sin(\theta_{in}) \text{ .... } \mathbf{(2)}$$

$$K_{spr} = \frac{2\pi}{\lambda} \times \sqrt{\frac{\varepsilon 1 \times \varepsilon 2}{\varepsilon 1 + \varepsilon 2}} \text{.... } \mathbf{(3)}$$

where n_p represents refractive index of prism, λ the wavelength of the light incident, θ_{in} indicates to the angle of incidence of laser beam, and ε1 and ε2 refers to dielectric steady of metal and sensing medium, respectively (Srivastava et al., 2011).

There are some criteria for the determination of resonance conditions such as the frequency of the incident light, the angle of incident and the metal medium refractive, the dielectric medium
and the sensing medium. The event angle is also regarded as the angle of resonance (Singh et al.,
2013).

Polarized light falls on the prism interface and the metal layer at a known angle of incidence and
is reflected depending on theory of total inner reflection;

- The reflectance of light has been measured via visual device dependence to stage investigation method, as a function of the angle of incidence with the wavelength of the incident light fixed.
- And according to the Wavelength investigation method so, when light is reflected can be measured as a function of light incident wavelength for steady incident angle.

A strong dip is showed in the resonance angle for the Phase investigation mode or resonance wavelength, and the refractive factor of the sensing medium can be resolved by knowing the resonance angle or resonance wavelength (Maharana et al., 2014).

2.1 Simulation of A Surface Plasmon Resonance Sensor: Methodology

In this study, a simulation program was constructed in MATLAB_b2018 by adopting the Fresnel equations of reflectivity of P-polarized electromagnetic wavelengths in range (100nm to 1000nm) and using the transfer matrix for a system consisting of brass layer with difference thicknesses (10 to 80) nm, changing 10 nm each time deposited on a prism of FD60_Dense glass, and the sensor is water in which the refractive index value has been changed by (Δn = 0, 0.03, 0.06, and 0.12). This plasmonic sensor system is as in Figure 2. The refractive index values of prism, brass, and water change as the wavelength of the light changes. Therefore, for the materials adopted in the plasmonic sensor system in this study, the values of the refractive indexes were used as a function of the wavelength from the tables available on site (https://refractiveindex.info). Numerical interpolation of the refractive index values was applied in order to obtain the refractive index values in the range of wavelengths from 100nm to 1000nm and then used in the simulation algorithm.

For the purpose of determining the resonance conditions, *p*-polarized (TM.) light must be used as any slight change in ε_d (water) leads to a transfer with the SPR dip curve (the reflectivity of light ray as a function to incident angle). The SPR sensitivity value will be given as follows (Fouad et al., 2016 ; Santos and Farahi, 2014):

$$S = \frac{\Delta\theta_{res}}{\Delta n} = \frac{\theta_{res1} - \theta_{res2}}{n_1 - n_2} \text{ ..... (4)}$$

$\Delta\theta_{res}$ indicate to the variation in resonance angle; and Δn refer to the variance of refractive factor in sensing medium (form n_1 to n_2), which leads to different in resonance angle. A large change in the resonance angle will increase the sensitivity of the SPR sensor.

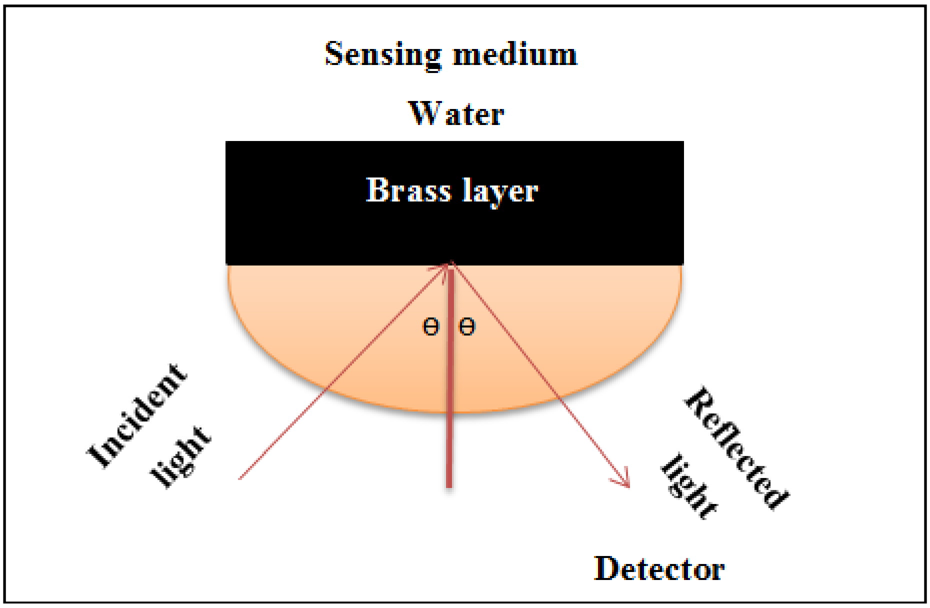

Figure 2. The proposed SPR sensor arrangement

The simulation process will calculate the sensor reflectivity as a function of changing the angle of incident light on a semicircular prism as the values of the angle of incidence are adopted within the range of 0 to 90 degrees, by using the values for the wavelengths varying from 100 nm to 1000 nm and using the refractive indices as a function of the wavelength. The position of the surface plasmon resonance dip will be determined.

The most important point in the simulation in order to determine the efficiency of the sensing system is to determine the effect of any slight change in the refractive index of the external sensor medium (water) on the surface plasmonic resonance angle. A slight change in the refractive index (Δn) values was used (0, 0.03, 0.06, and 0.12).

3. RESULTS AND DISCUSSIONS

The sensor reflectivity in Figure 3 as a function of the incident light angle to the interface between the sensing layers and the prism was obtained by implementing MATLAB simulation algorithm. When the wavelengths were changed from 100 nm to 1000 nm and the thickness of the brass layer changed from 10 nm to 80 nm, the curves obtained cannot observed SPR dips at wavelengths from 100 nm to 1000 for brass layer thickness 10 nm, also the curves cannot observed SPR dips at wavelengths from 100 nm to 800 for brass layer thickness 20nm and weak peaks in wavelengths 900 and 1000 nm. Furthermore, the curves cannot observed

SPR dips at wavelengths from 100 nm to 500 nm for brass layer thickness from 30 nm to 80 nm. However, SPR dips were appeared weakly at visible region 600 nm and 700nm, at brass thicknesses from 30nm to 70nm, and the SPR dip almost disappears at brass thickness 80nm. The curves too cannot observed SPR dips at wavelengths 800 nm for brass layer thickness of 10nm to 80nm, while a strong appearance of SPR was observed in the infrared region of 900 nm and 1000 nm at a brass layer with thicknesses of 30nm-50nm and a weak at thickness of 60 nm and almost disappeared at thicknesses of 70nm and 80nm.

In this study, the reflectivity curves were analyzed to determine the sensor parameters for each wavelength and brass thickness. Both the full width at half maximum (FWHM) and the length (H) of the SPR dip was calculated only for the wavelengths (700nm, 900nm, and 1000nm) in which the plasmonic resonance appeared. These values were calculated as a function of the thickness of the brass layer then plotted as shown in the Figure 4 and 5.The sensitivity of the proposed SPR sensor system was also calculated as a function of the change in the thickness of the brass layer, and its results are shown in the Figure 6.

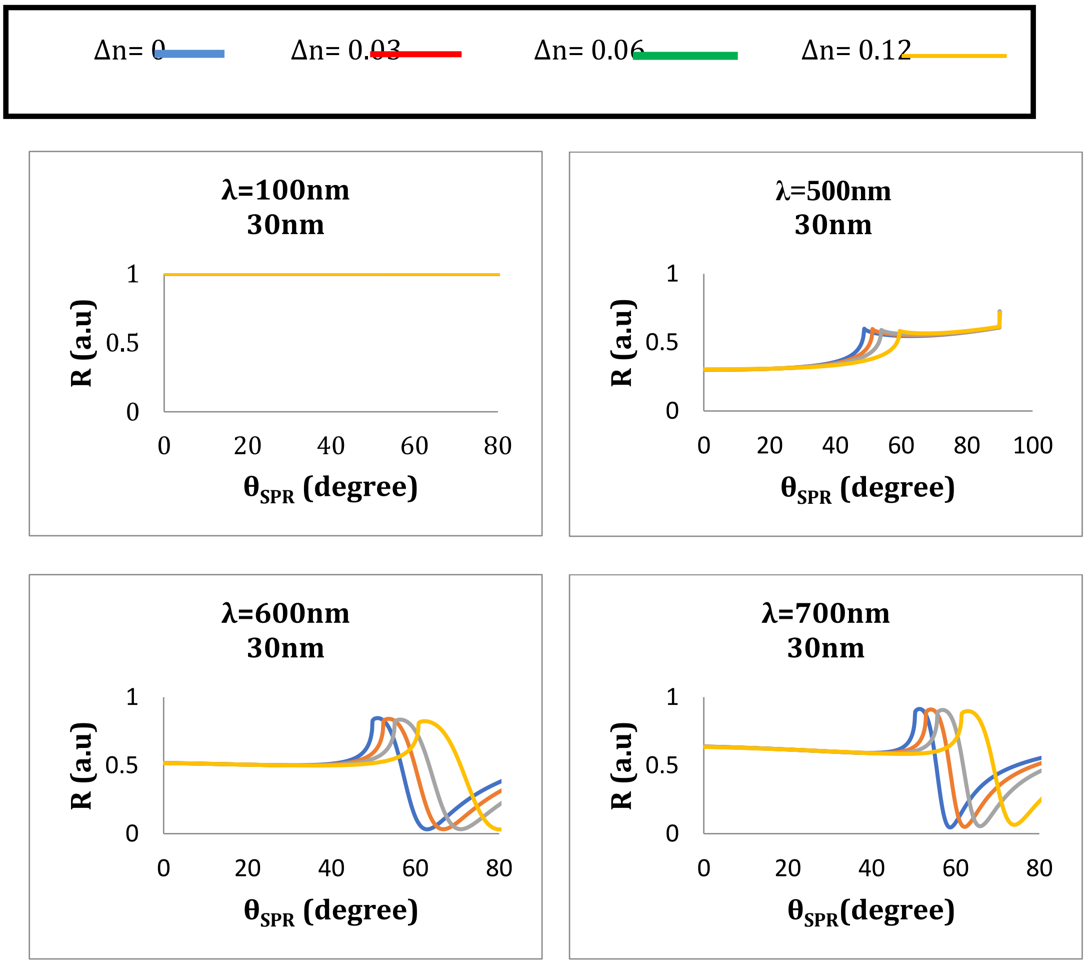

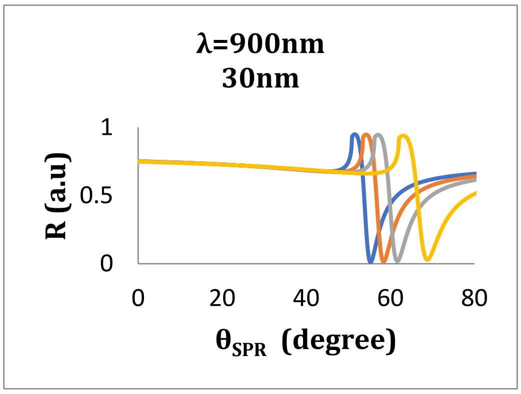
λ=900nm
30nm
R (a.u)
1
0.5
0
0
20
40
60
80
θSPR (degree)

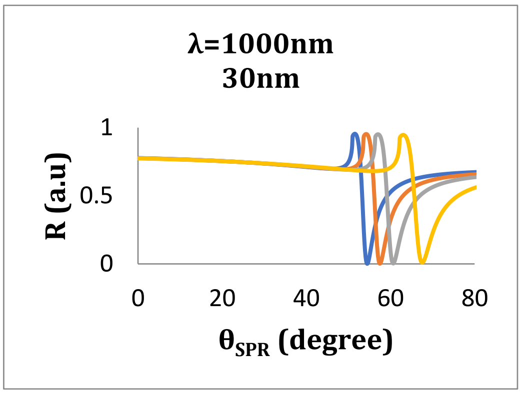
λ=1000nm
30nm
R (a.u)
1
0.5
0
0
20
40
60
80
θSPR (degree)

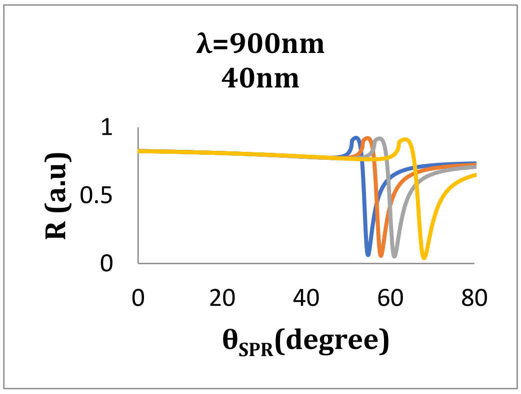
λ=900nm
40nm
R (a.u)
1
0.5
0
0
20
40
60
80
θSPR(degree)

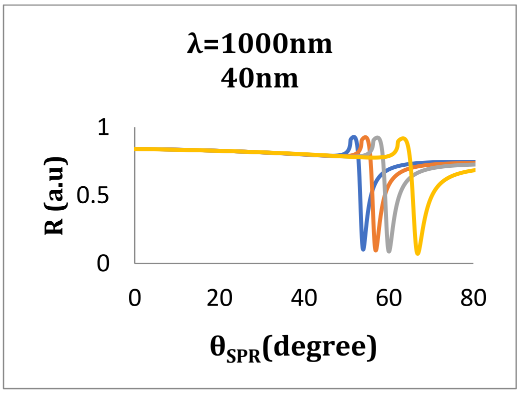
λ=1000nm
40nm
R (a.u)
1
0.5
0
0
20
40
60
80
θSPR(degree)

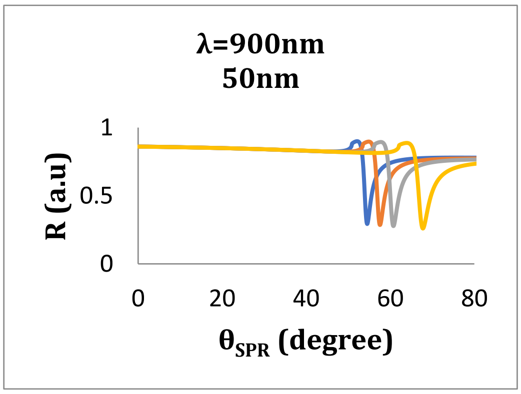
λ=900nm
50nm
R (a.u)
1
0.5
0
0
20
40
60
80
θSPR (degree)

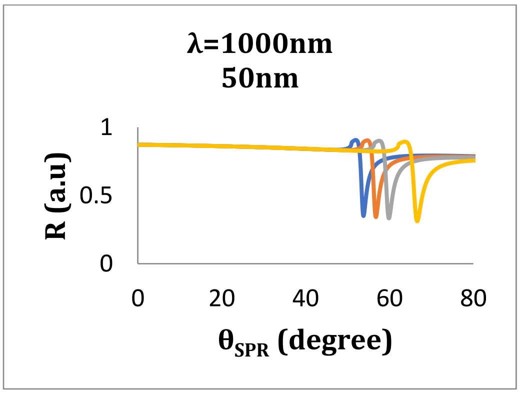
λ=1000nm
50nm
R (a.u)
1
0.5
0
0
20
40
60
80
θSPR (degree)

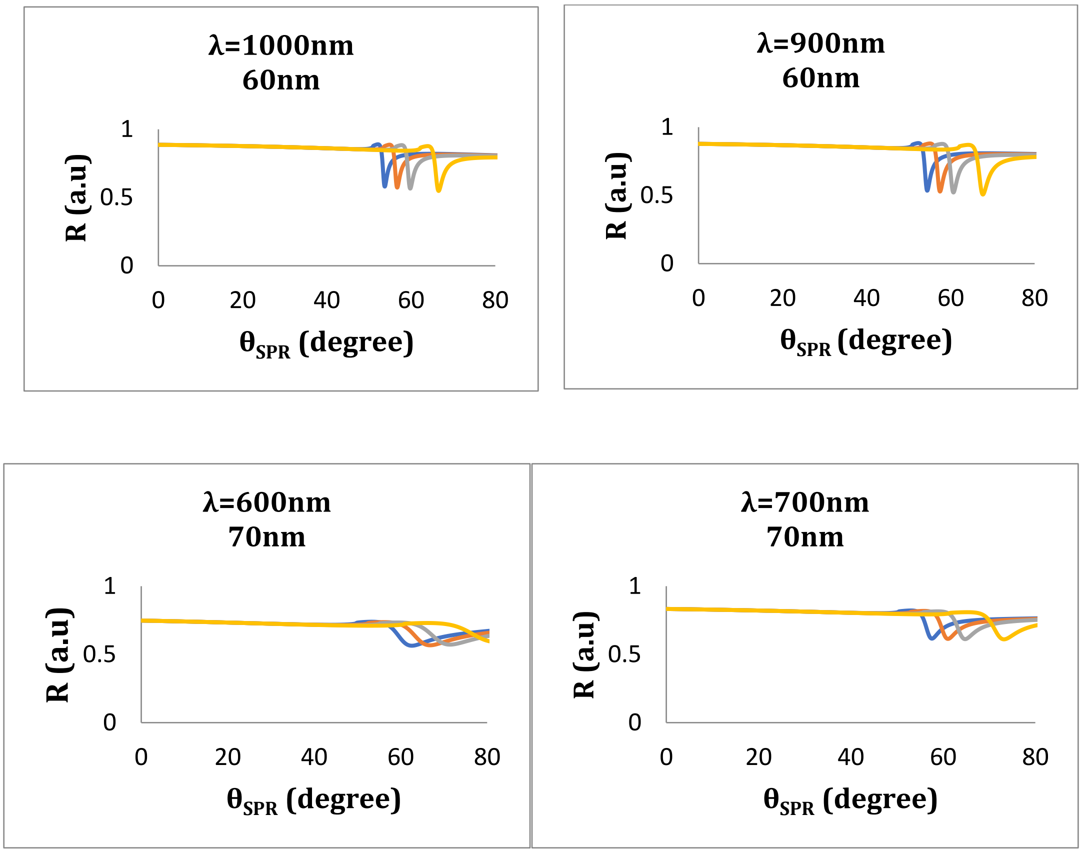

Figure 3. Surface plasmon resonance sensor for thickness 10-80 nm at wavelengths 100 -1000 nm

Figure 4 shows that FWHM was inversely proportional to increasing the thickness of the brass layer in the visible and infrared regions, and the best FWHM values were obtained in the infrared region, where the SPR dip was more narrow, and it was also noted that the FWHM values improved and became more narrow as the thickness of the brass layer increases. As for the SPR dipping length (H) in Figure 5, as the brass layer thickens in the visible and infrared regions, it begins to gradually decrease with the increase in the thickness of the brass and its best values are at the thickness from 20 nm to 40 nm. As for the results of the sensitivity values obtained for this sensing system, they were as in the Figure. It is noticed, that the best values obtained were in the visible region at the wavelength of 700nm, where it was almost stable with an increase in the thickness of the brass layer from 20nm to 50nm and with values higher than 115 deg/RIU. While in the infrared region, the sensitivity was between (100 to 103) deg/RIU and almost stable for brass layer thicknesses from about 20nm to 60nm.

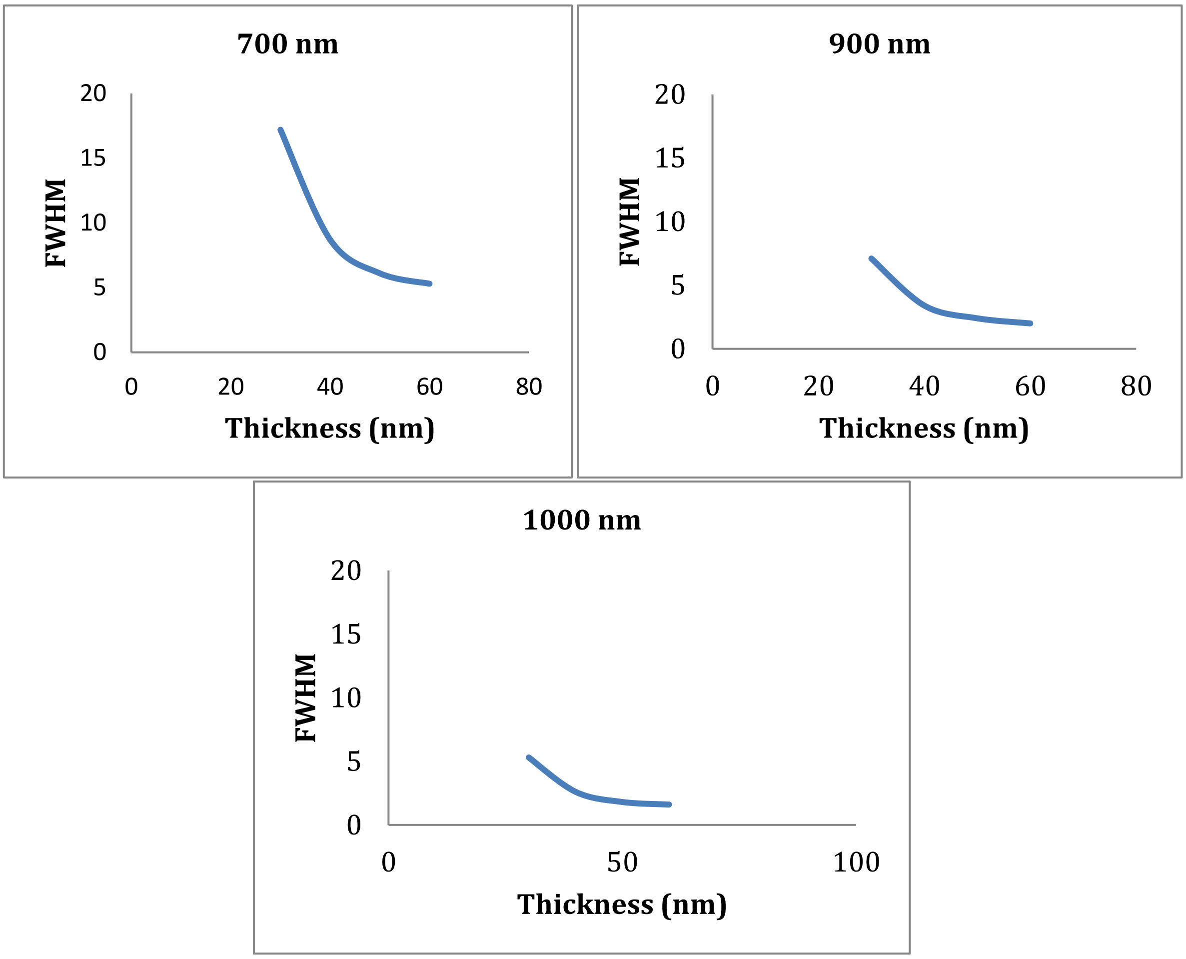

Figure 4. FWHM for thickness 10-80nm at wavelengths 100-1000 nm

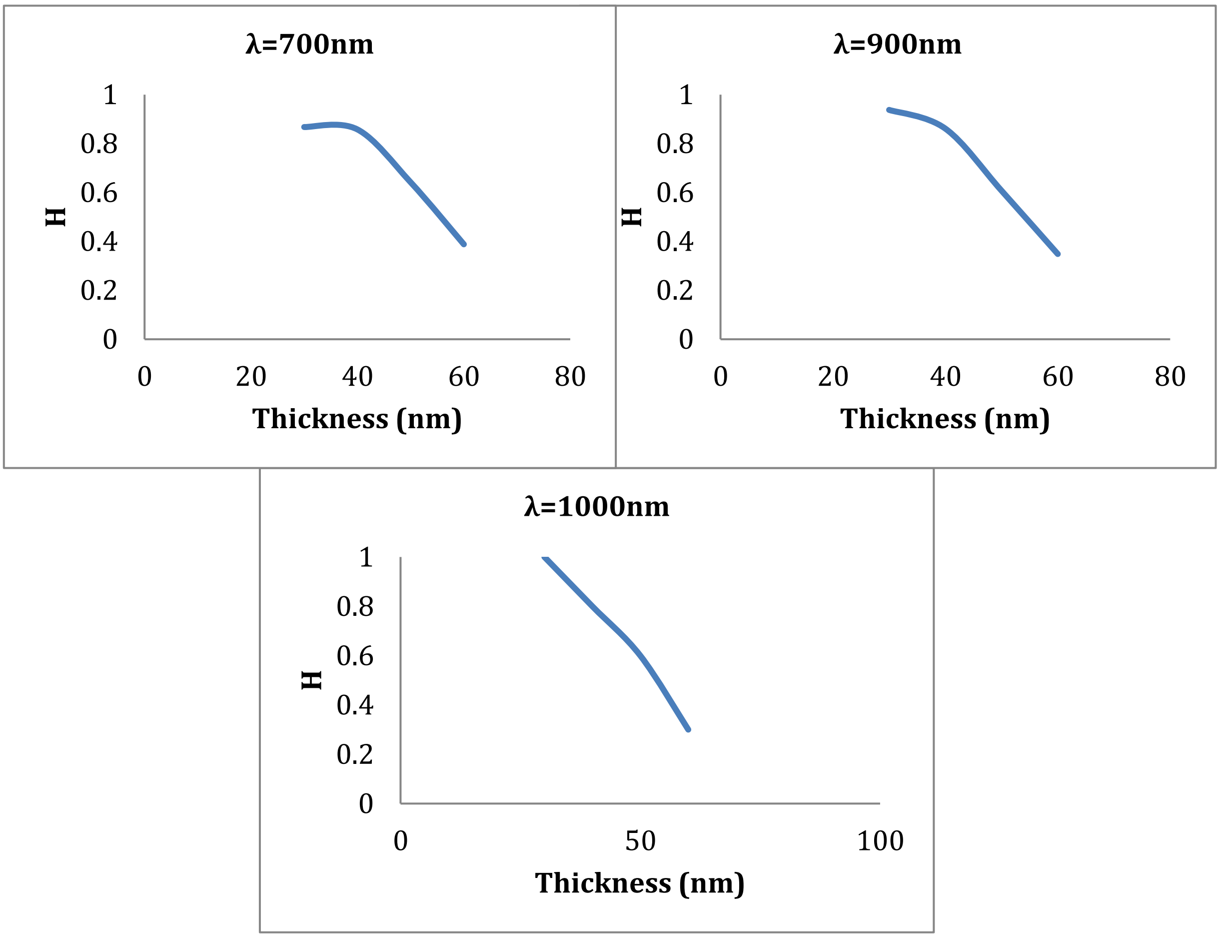

Figure 5. The length (H) of the SPR dip for thickness 10 -80 nm at wavelengths 100 -1000 nm

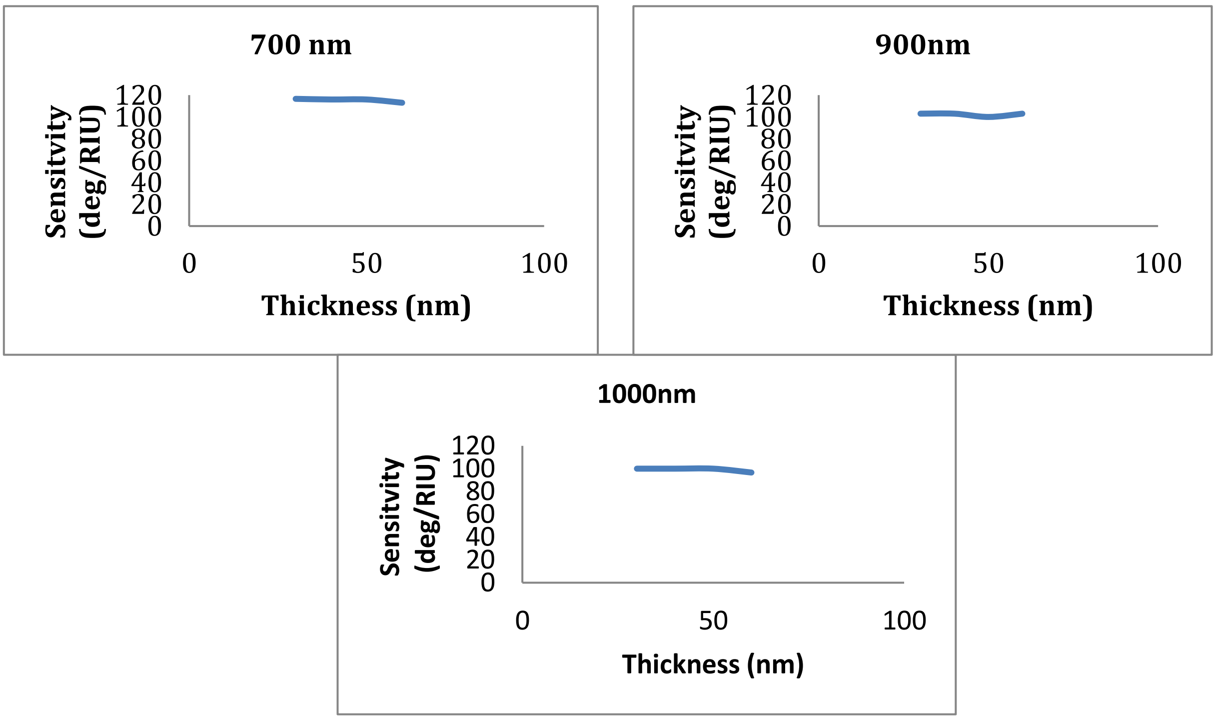

Figure 6. Sensitivity of sensor for thickness 10 - 80nm at wavelengths100-1000 nm

4. CONCLUSIONS

From the suggested SPR sensor simulation results, the following points canbe concluded:

1. There is no SPR in the wavelengths range 100-500 nm for brass layer thickness from 10 nm to 80 nm.
2. SPR dips were appeared weakly at visible region 600nm and 700nm, at brass thicknesses from 30nm to 70nm, and the SPR dip almost disappears at brass thickness 80nm.
3. A strong appearance of SPR was observed in the infrared region (900 nm and 1000 nm) at a brass layer with thicknesses of 30nm-50nm and a weak at thickness of 20nm and 60nm and almost disappeared at thicknesses 80nm.
4. FWHM values improved and became narrower as the thickness of the brass layer increases, while the values of the SPR dip length (H) decreases with the increase in the thicknesses of brass layer.
5. The best sensitivity values appeared at the wavelength of 700nm, where the system showed a sensitivity of approximately 115 deg/RIU stable for the values of the brass thicknesses between 20nm to 50nm.
6. Whereas at wavelengths 900nm and 1000nm, the sensitivity drops to the range of about 100 deg/RIU, but the SPR sensor was more stable in brass layer thicknesses from 20nm to 60nm.
7. Finally, the optimum thickness of the brass layer that can be used in the proposed SPR sensor can be determined to work with high stability, which should be within the limits of values between 20nm and 40nm. As FWHM values, the length (H) and sensor sensitivity are at their best, and for the three wavelengths 700nm, 900nm and 1000nm.

References

FOUAD, S., NASEER, S., JAMAL, Z. & POOPALAN, P. 2016. Enhanced sensitivity of surface plasmon resonance sensor based on bilayers of silver-barium titanate. *Журнал нано-та електронної фізики*, 04085-1-04085-5.

FOUAD, S., SABRI, N., JAMAL, Z. & POOPALAN, P. 2017. Surface plasmon resonance sensor sensitivity enhancement using gold-dielectric material. *Int. J. Nanoelectronics and Materials,* 10, 149-158.

GHOSH, S. & RAY, M. 2015. Analysis of silicon based surface Plasmon Resonance Sensors with different amino acids. *Silicon,* 7, 313-322.

KITA, S., NISHIJIMA, Y., MISAWA, H. & BABA, T. Label-free biosensing utilizing ultrasmall photonic crystal nanolaser. Integrated Photonics and Nanophotonics Research and Applications, 2009. Optical Society of America, IMB3.

Kadhum, F.J., Kafi, S.H., Saeed, A.A., Al-Zuky, A.A. and Al-Saleh, A.H. (2021). Simulation of Surface Plasmon Resonance (SPR) of Silver with Titanium Oxide as a Bi-Layer Biosensor. *The Scientific Journal of King Faisal University: Basic and Applied Sciences*, **22**(2), Page Numbers. DOI: 10.37575/b/sci/210046.

LIN, Z., CHEN, S. & LIN, C. 2020. Sensitivity improvement of a surface plasmon resonance sensor based on two-dimensional materials hybrid structure in visible region: a theoretical study. *Sensors,* 20, 2445.

MAHARANA, P. K., JHA, R. & PALEI, S. 2014. Sensitivity enhancement by air mediated graphene multilayer based surface plasmon resonance biosensor for near infrared. *Sensors and Actuators B: Chemical,* 190, 494-501.

NISHA, A., MAHESWARI, P., ANBARASAN, P., RAJESH, K. & JAROSZEWICZ, Z. 2019. Sensitivity enhancement of surface plasmon resonance sensor with 2D material covered noble and magnetic material (Ni). *Optical and Quantum Electronics,* 51**,** 19.

ROBERTSON, W. & MAY, M. 1999. Surface electromagnetic wave excitation on one-dimensional photonic band-gap arrays. *Applied physics letters,* 74**,** 1800-1802.

SANTOS, J. L. & FARAHI, F. 2014. *Handbook of optical sensors*, Crc Press.

SHUKLA, S., SHARMA, N. K. & SAJAL, V. 2015. Sensitivity enhancement of a surface plasmon resonance based fiber optic sensor using ZnO thin film: a theoretical study. *Sensors and Actuators B: Chemical,* 206**,** 463-470.

SINGH, S., MISHRA, S. K. & GUPTA, B. D. 2013. Sensitivity enhancement of a surface plasmon resonance based fibre optic refractive index sensor utilizing an additional layer of oxides. *Sensors and Actuators A: Physical,* 193**,** 136-140.

SRIVASTAVA, T., DAS, R. & JHA, R. 2011. Highly accurate and sensitive surface plasmon resonance sensor based on channel photonic crystal waveguides. *Sensors and Actuators B: Chemical,* 157**,** 246-252.

SU, W., ZHENG, G. & LI, X. 2013. A resonance wavelength easy tunable photonic crystal biosensor using surface plasmon resonance effect. *Optik,* 124**,** 5161-5163.

WANG, F., CHEN, C., MAO, P., LUO, Y., CHEN, X., FANG, J., PENG, S., ZHANG, J., TANG, J. & LU, H. Sensitive surface plasmon resonance biosensor based on a photonic crystal and bimetallic configuration. Numerical Simulation of Optoelectronic Devices, 2014, 2014. IEEE, 117-118.

XU, H., WU, L., DAI, X., GAO, Y. & XIANG, Y. 2016. An ultra-high sensitivity surface plasmon resonance sensor based on graphene-aluminum-graphene sandwich-like structure. *Journal of Applied Physics,* 120**,** 053101.